

Variable amplitude fatigue studies on steel beams

Autor(en): **Heins, Conrad P. / Murad, Francis A.**

Objektyp: **Article**

Zeitschrift: **IABSE publications = Mémoires AIPC = IVBH Abhandlungen**

Band (Jahr): **31 (1971)**

PDF erstellt am: **16.08.2024**

Persistenter Link: <https://doi.org/10.5169/seals-24219>

Nutzungsbedingungen

Die ETH-Bibliothek ist Anbieterin der digitalisierten Zeitschriften. Sie besitzt keine Urheberrechte an den Inhalten der Zeitschriften. Die Rechte liegen in der Regel bei den Herausgebern.

Die auf der Plattform e-periodica veröffentlichten Dokumente stehen für nicht-kommerzielle Zwecke in Lehre und Forschung sowie für die private Nutzung frei zur Verfügung. Einzelne Dateien oder Ausdrucke aus diesem Angebot können zusammen mit diesen Nutzungsbedingungen und den korrekten Herkunftsbezeichnungen weitergegeben werden.

Das Veröffentlichen von Bildern in Print- und Online-Publikationen ist nur mit vorheriger Genehmigung der Rechteinhaber erlaubt. Die systematische Speicherung von Teilen des elektronischen Angebots auf anderen Servern bedarf ebenfalls des schriftlichen Einverständnisses der Rechteinhaber.

Haftungsausschluss

Alle Angaben erfolgen ohne Gewähr für Vollständigkeit oder Richtigkeit. Es wird keine Haftung übernommen für Schäden durch die Verwendung von Informationen aus diesem Online-Angebot oder durch das Fehlen von Informationen. Dies gilt auch für Inhalte Dritter, die über dieses Angebot zugänglich sind.

Variable Amplitude Fatigue Studies on Steel Beams

Essai de fatigue sur des poutres métalliques sous l'effet d'amplitudes variables

Ermüdungsversuche an Stahlträgern mit variabler Amplitude

CONRAD P. HEINS

Associate Professor, Civil Engineering
Department, University of Maryland,
College Park, Md., U.S.A.

FRANCIS A. MURAD

Research Graduate Assistant, Civil Engi-
neering Department, University of Mary-
land, College Park, Md., U.S.A.

Introduction

An extensive research program has been initiated in the United States, to obtain field loading history data and the resulting effects on bridge structures [1], [2], [3], [4].

The collection of these data [5], [6], [7], [8] will then permit simulated laboratory studies on various bridge elements.

It is the purpose of this paper to present the results of such a laboratory study, and a proposed fatigue damage hypothesis which considers random loadings. The theory and experiments will only consider steel beams with welded cover plates.

Theory

The fatigue life of a specimen, subjected to stress cycles at varying amplitudes, requires a damage index. Crack growth data might be considered as such an index. However, the difficulty in measuring this phenomenon is difficult if not impossible. An alternate index, which is measurable, is the accumulated plastic strain, which will be utilized in this study.

Stress-Cycle Criteria. Examination of crack growth data [1], [10] indicates that the growth rate is exponential with respect to cycles. Assuming strain accumulation and crack growth behave similarly, the following Eq. (1) is proposed:

$$\frac{d\epsilon_p}{dn} = A \alpha \sigma_r^\gamma n^{\alpha-1}, \quad (1)$$

where A , α and γ are stress dependent material constants, which are to be determined experimentally. The term σ_r represents the stress range which was demonstrated (11) to be the significant parameter in fatigue of steel beams with cover plates.

The total plastic strain at n cycles is:

$$\epsilon_p = A \sigma_r^\gamma n^\alpha \quad (2)$$

and at failure N_f is:

$$\epsilon_f = A \sigma_r^\gamma N_f^\alpha. \quad (3)$$

Eq. (3) can be described in logarithm form as follows, thus representing a typical $\sigma_r - N_f$ diagram.

$$\text{Log } N_f = \frac{1}{\alpha} \text{Log} \left(\frac{\epsilon_f}{A} \right) - \frac{\gamma}{\alpha} \text{Log } \sigma_r \quad (4)$$

or

$$\text{Log } N_f = b - c \text{Log } \sigma_r \quad (5)$$

where:

$$b = \frac{1}{\alpha} \text{Log} \left(\frac{\epsilon_f}{A} \right), \quad c = \frac{\gamma}{\alpha}.$$

Damage Criteria. The rate of damage, as indicated previously, will be reflected on the amount of accumulated strain, or

$$D = \left(\frac{\epsilon_p}{\epsilon_f} \right). \quad (6)$$

Substituting Eqs. (2) and (3) into (6) gives:

$$D = \left(\frac{n}{N_f} \right)^\alpha, \quad (7)$$

where α is a function of the stress range (σ_r), and at failure the value of D will equal one.

Required Coefficients. In order to apply Eqs. (5) and (7), particular coefficients are required. The coefficients b and c of Eq. (5) can be obtained from constant amplitude tests and represent the intercept and slope of a curve of the diagram.

The variable α can be established by obtaining the strain accumulation per cycle $\left(\frac{d\epsilon}{dn} \right)$ Eq. (1) and plotting these data on Log-Log paper vs. n , for the respective stress ranges. This will yield an equation of the form:

$$\text{Log} (\alpha - 1) = d - e \text{Log } \sigma_r, \quad (8)$$

where d and e are constants to be determined experimentally.

Variable Amplitude Analysis. In order to apply the above equations, the damage accumulation process is assumed to be interaction-free. That is, the application of other stress amplitudes will not alter the damage curves established from constant amplitude data. This can be illustrated by examining Fig. 1, where three specimens accumulate damage equal to (D) , resulting from

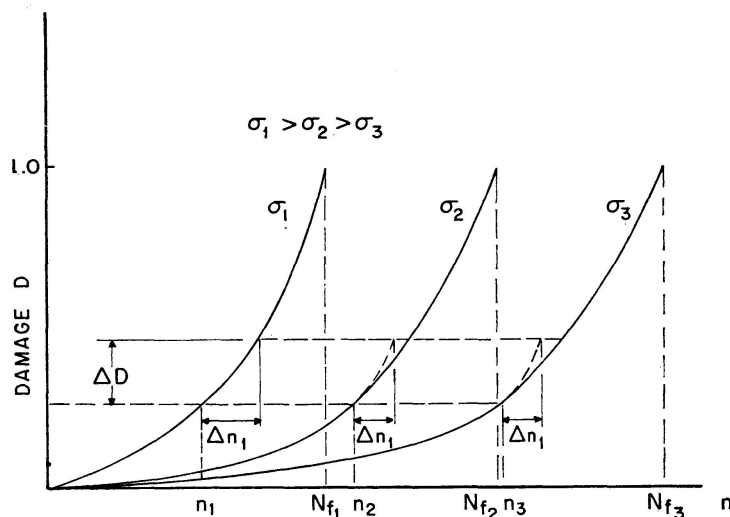


Fig. 1. Hypothetical Damage-Cycle Relationship.

application of stresses and cycles of (σ_1, n_1) ; (σ_2, n_2) ; and (σ_3, n_3) . If the application of an additional (Δn_1) cycle at stress range (σ_1) occurs to any of the specimens, an increment of damage equal to (ΔD) results. The path of the damage curves for all three specimens will be the same as that for specimens loaded at (σ_1) range, and is shown dotted in Fig. 1.

Because the three specimens have equivalent damage, an expression relating the effective cycles at one level (i) to another level $(i+1)$ is formulated as follows:

$$D_i = D_{i+1}$$

and from Eq. (7):

$$\left(\frac{n_i}{N_{fi}}\right)^{\alpha_i} = \left(\frac{n_{i+1}}{N_{fi+1}}\right)^{\alpha_{i+1}}, \quad (9)$$

$$n_{i+1} = N_{fi+1} \left(\frac{n_i}{N_{fi}}\right)^{\alpha_i/\alpha_{i+1}}. \quad (10)$$

With the basic Eqs. (5), (7), (8) and (10) established, the analysis of members subjected to variable amplitude loads can be performed.

Example. Consider a member subjected to (σ_1, n_1) and (σ_2, n_2) stresses and cycles. It is required to determine the number of cycles (n_3) at stress range (σ_3) to cause failure. Fig. 2 describes the loading pattern.

The following will outline the required calculations, with the results presented graphically in Fig. 3.

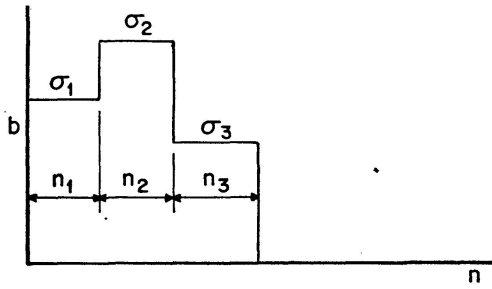


Fig. 2. Stress-Cycle Pattern.

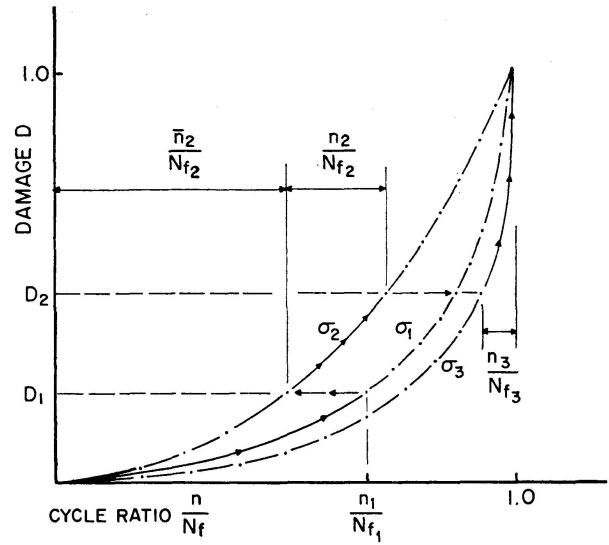


Fig. 3. Damage Accumulation due to Variable Amplitude Loads.

1. Calculate the cycles to failure at the respective stress ranges from Eq. (5) (N_{f1}, N_{f2}, N_{f3}).
2. Evaluate the variable α at the respective stress ranges from Eq. (8) ($\alpha_1, \alpha_2, \alpha_3$).
3. Evaluate damage D_1 due to (n_1) cycles at stress range (σ_1), from Eq. (7).
4. Determine equivalent cycle ratio ($\frac{\bar{n}_2}{N_{f2}}$) producing damage equal to D_1 . Apply Eq. (9), which gives

$$\left(\frac{\bar{n}_2}{N_{f2}}\right) = \left(\frac{n_1}{N_{f1}}\right)^{\alpha_1/\alpha_2}$$

5. Evaluate the total damage D_2 , due to previous loading (σ_1, n_1) and present loading (σ_2, n_2). Eq. (10) gives:

$$D_2 = D_1 + \Delta D_2 = \left(\frac{\bar{n}_2}{N_{f2}} + \frac{n_2}{N_{f2}}\right)^{\alpha_2}$$

6. Determine equivalent cycle ratio ($\frac{\bar{n}_3}{N_{f3}}$) providing damage equal to D_2 . Apply Eq. (9), which gives:

$$\left(\frac{\bar{n}_3}{N_{f3}}\right) = \left(\frac{\bar{n}_2}{N_{f2}} + \frac{n_2}{N_{f2}}\right)^{\alpha_2/\alpha_3}$$

7. The number of cycles (n_3) at stress range (σ_3) that can be sustained up until failure is equal to:

$$n_3 = N_{f3} - \bar{n}_3$$

The above example demonstrates the application of the proposed equations. These equations can be applied to any pattern of stress levels and any number. A computer program has been written [12] to apply these equations when a large number of stress-cyclic levels are encountered.

Constant Amplitude Tests

Specimen. As shown in Fig. 4, the test specimen was a 12 WF 27 beam with a $5'' \times 3/8'' \times 8' - 0''$ welded cover plate, all of ASTM A 36 steel. Strain gages to measure strain accumulation were positioned on top of the bottom flange, at the ends of the cover plates. Additional gages, as shown, were used to monitor load application.

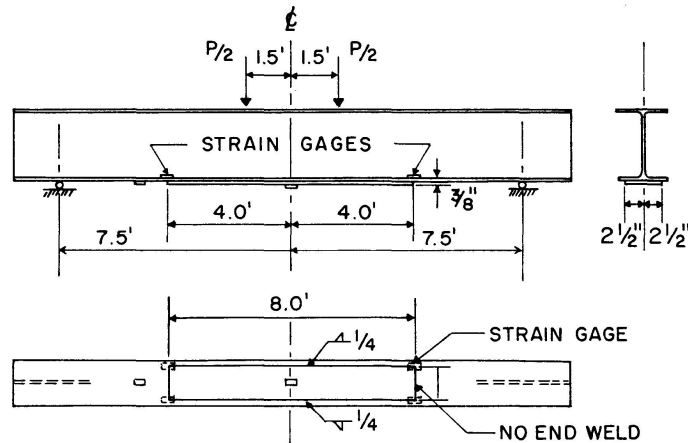


Fig. 4. Test Specimen.

Standard tension tests of coupons taken from the web, flange and cover plate of the test specimens produced an average value of 30.0×10^3 ksi for the Modulus of Elasticity.

Equipment. The fatigue testing equipment consisted of a closed loop hydraulic system with a 20 gpm pump. The accumulator has a 50 kip dynamic load capacity.

Ten block programming modules provide the system with the ability to generate a predetermined number of cycles at a certain mean and dynamic amplitude level at various frequencies.

Test Program. As described in Table 1, eleven specimens were tested at constant amplitude. Strain accumulation data was obtained throughout these tests [12].

Test Results. Table 2 describes the constant amplitude test results. Indicated in this table are the cycles to failure of the strain gage which is when the first visible crack appears and when the specimen completely fails or ruptures.

A plot of the cycles to failure, dictated by the gage, and stress range at the cover plate are given in Fig. 5. A least square fit of these data gives:

$$\text{Log } N_f = 9.158 - 2.98 \text{ Log } \sigma_r. \quad (11)$$

This equation is similar to Eq. (5), as was previously described.

In addition to obtaining cycles to failure, strain accumulation data were collected. The data $\left(\frac{d\epsilon}{dn}\right)$ vs. n for specimens CA-1 through CA-9 is given in

Table 1. Constant Amplitude Test Program

Specimen	Minimum Stress - ksi		Stress Range - ksi		Maximum Stress-ksi Centerline
	Centerline	End of C.P.	Centerline	End of C.P.	
CA-1	5.00	4.35	15.00	13.04	20.00
CA-2	5.00	4.35	15.00	13.04	20.00
CA-3	5.00	4.35	15.00	13.04	20.00
CA-4	5.00	4.35	10.75	9.35	15.75
CA-5	5.00	4.35	10.75	9.35	15.75
CA-6	5.00	4.35	20.00	17.40	25.00
CA-7	5.00	4.35	20.00	17.40	25.00
CA-8	2.00	1.75	25.00	21.75	27.00
CA-9	2.00	1.75	25.00	21.75	27.00
CA-10	5.00	4.35	9.00	7.82	14.00
CA-11	5.00	4.35	8.00	7.00	13.00

Table 2. Constant Amplitude Test Results

Specimen Number	Stress Range ksi AT C.P.	Number of Cycles to Failure of Gage	Number of Cycles to Failure of Specimen
CA-1	13.04	1,721,500	1,907,860
CA-2	13.04	1,585,200	1,787,200
CA-3	13.04	NA	873,300
CA-4	9.35	644,500	703,700
CA-5	9.35	518,950	582,300
CA-6	17.40	295,540	313,800
CA-7	17.40	264,600	286,800
CA-8	21.75	138,700	151,550
CA-9	21.75	144,450	157,600
CA-10	7.82	3,109,000*	—
CA-11	7.00	4,100,000*	—

NA = not operable. * Runout no strain accumulation.

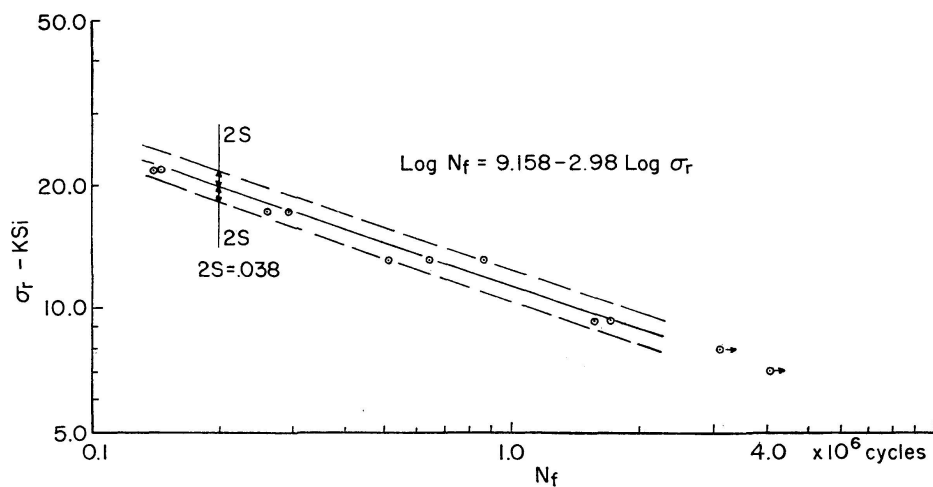


Fig. 5. Stress Range vs. Cycles to Failure.

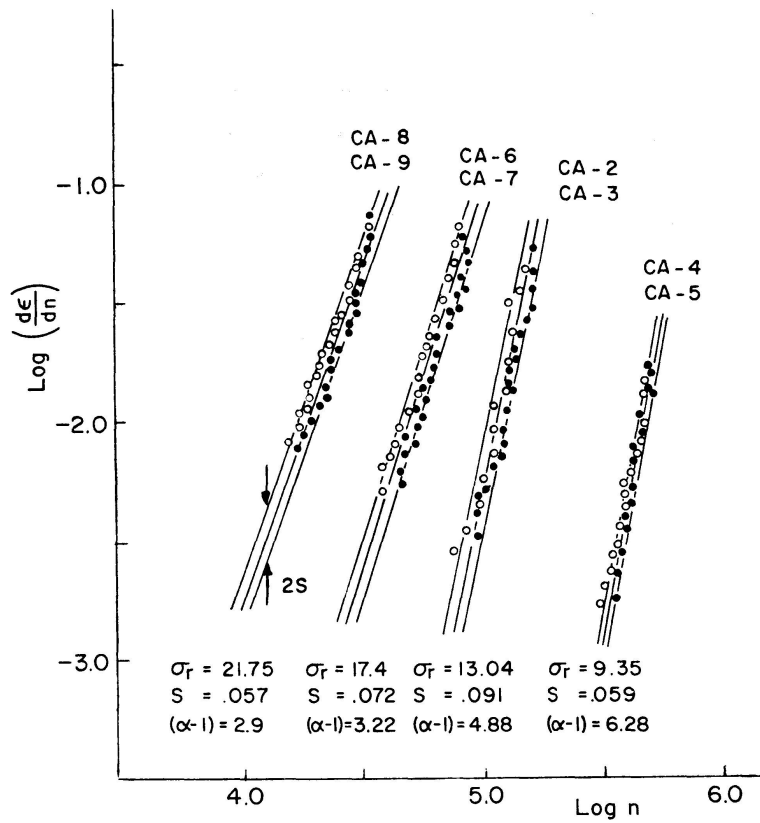


Fig. 6. Strain Accumulation per Cycle vs. Equivalent Number of Cycles.

Fig. 6. A regression line has been established for each specimen, and the respective slope (α-1) determined. A plot of these slopes vs. the stress range σ_r is given in Fig. 7. A least square fit of these data gives the following equation:

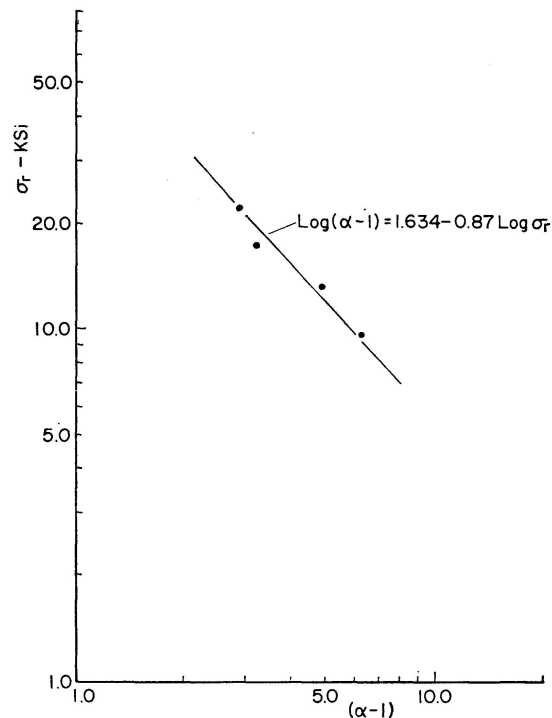


Fig. 7. (α-1) vs. Stress Range.

$$\text{Log}(\alpha - 1) = 1.634 - 0.87 \text{Log} \sigma_r. \quad (12)$$

This equation is similar to Eq. (8), as described previously.

It should be noted that Eq. (11) has been substantiated by the test results obtained at Lehigh University [11]. These tests, however, consisted of some 35 beam specimens and the failure criteria was specimen failure and not gage failure, yielding some slight variations in the $\sigma_r - N_f$ equation.

Variable Amplitude Tests

Test Program. In order to check the validity of the theory, a series of random load tests were conducted. The endurance of the test specimen and strain accumulation was obtained during these tests.

The applied stress and number of cycles, for specimens VAMST 1 through VAMST 4, was selected to represent approximately 20% of the constant amplitude cycles which caused failure. The order of loading consisted of two random, one high to low and one low to high, as described in Fig. 8. The two random loadings, VAMST 1 and 2, consisted of nine block loadings obtained by subdividing the cyclic blocks, given in Fig. 8, except for stress level 13.0 ksi. Specimens VAMST 3 and 4 loadings are as shown in Fig. 8.

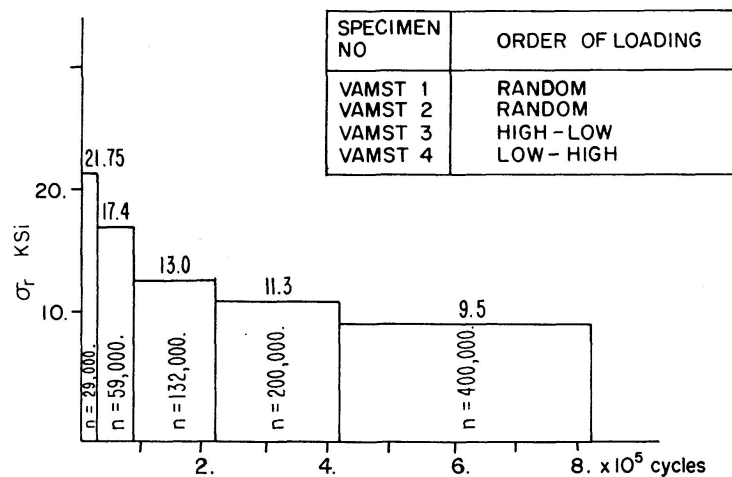


Fig. 8. Variable Amplitude Multi-Step Tests 1-4.

An additional load pattern was selected, Fig. 9, from actual field test data (8). The load factor used was 4.0, as the field data consisted of maximum stress range of 6.0 ksi. The number of consecutively applied cycles, as given by the field data, was also increased 300 times, to examine the effects of a large number of consecutive cycles. Additional tests of this type have also been conducted [12], and yield similar results, now to be presented.

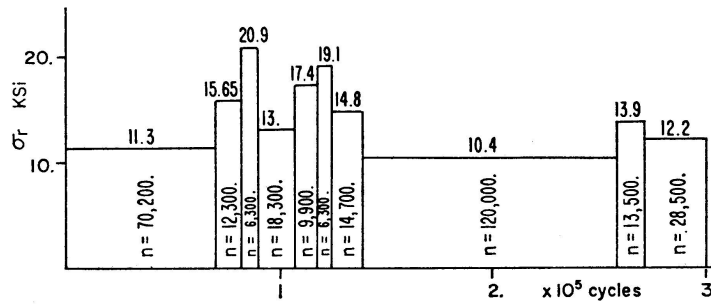


Fig. 9. Variable Amplitude Multi-Step Test 5.

Test Results. As described in Fig. 8, the cover plated specimens were subjected to five varying stress levels at a specific number of cycles per level. The first two specimens, VAMST 1 and VAMST 2, were subjected to a random set of these stress range levels. The random pattern selected resulted in the following order of stress range levels: $\sigma_r = 9.5, 21.75, 17.4, 11.3, 13.0, 11.3, 9.5, 17.4, 21.75, 9.5$. Specimen VAMST 1, had gage failure in the ninth block at a stress range level of 21.75 ksi. Specimen VAMST 2, gage failed in the tenth block at stress range level of 9.5 ksi. The total number of cycles at failure are given in Table 3.

Table 3. Variable Amplitude Multi-Step Test Results

Specimen Number	Number of Cycles at Failure of Gage	Number of Cycles at Failure of Specimen	Stress Range at Failure of Gage - ksi	Number of Blocks at Gage Failure
VAMST 1	819,500	980,000	21.75	9
2	889,500	1,023,000	9.50	10
3	650,000	825,400	9.50	5
4	1,451,000	1,516,000	13.00	8
5	866,500	978,205	13.90	29

Specimen VAMST 3, was subjected to a high to low stress level of loading. This specimen failed after application of the fifth stress level ($\sigma_r = 9.5$ ksi) or fifth block, as listed in Table 3.

Specimen VAMST 4, which was subjected to a low to high stress pattern as given in Fig. 8, had failure of the gage during the eighth block loading ($\sigma_r = 13.0$ ksi). This specimen was, therefore, subjected to one complete loading pattern (5 blocks), with initiation of 3/5 of a similar pattern. Table 3, describes the accumulative number of cycles absorbed by this specimen. The order of loading and resulting cycles to failure is most apparent in comparing this data with specimen VAMST 3 data.

Specimen VAMST 5, which was subjected to stress levels and cyclic variations representing actual field data had gage failure after 29 block loadings. The stress level at gage fail was 13.9 ksi, as listed in Table 3.

Comparison with Theory. A comparison between the experimental data and the proposed theory and theories by MINER [13] and HENRY [14], are given in Table 4. The predicted number of cycles to failure, according to the three theories, shows that all three theories are conservative. A comparison between block ratios, n/N_f , at the failure block are also listed.

Table 4. Comparison of VAMST Results with Theory

Spec. No.	Acc. No. of Cycles to Fall	Stress Level at Failure of Gage ksi	Calculated Cum. No. of Cycles			Failure Block Ratio	
			Theory	Miner	Henry	Theory \bar{n}/N_f	Miner n/N_f
VAMST 1	819000	21.75	809100	775000	672500	1.01	1.01
2	889000	9.5	809100	775000	672500	1.05	1.05
3	650000	9.5	450000	816600	615000	1.10	0.91
4	1451000	13.0	980000	816600	898000	1.14	1.52
5	866500	15.9	701000	709300	660000	1.13	1.16

N_f = number of constant amplitude cycles at last stress level to cause failure.
 \bar{n} = calculated number of cycles at last stress level to induce final failure damage.
 n = given number of cycles at calculated stress failure level.

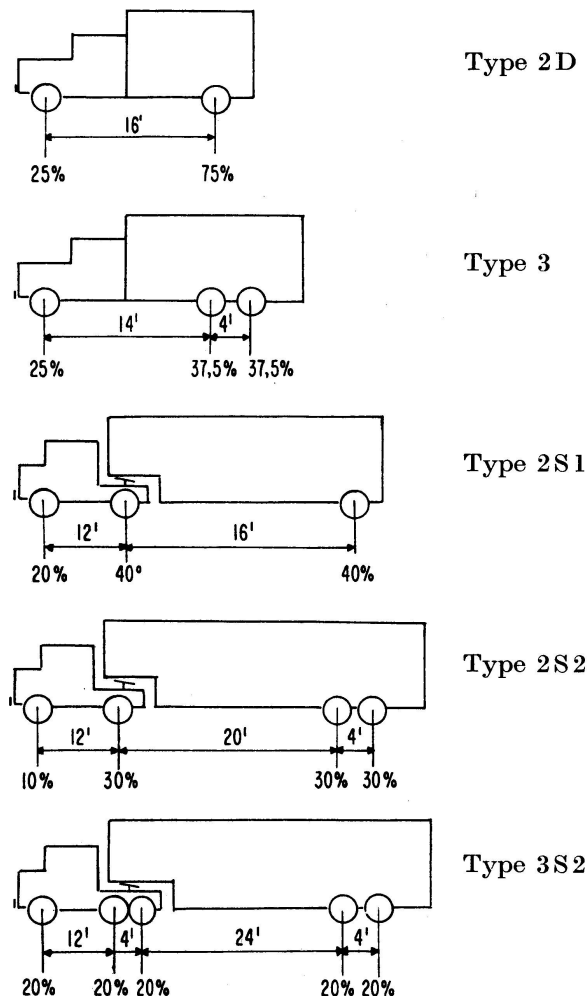


Fig. 10. Truck Types.

Application

Truck Classifications. Examination of extensive field data [5], [6], [7], [8] has resulted in five typical truck types, as given in Fig. 10. The distribution of axle weight and axle spacings are typical for the present traffic trends.

Maximum Moments. The maximum moments induced in a simply supported beam, due to these moving loads, have been calculated assuming gross weight equal to 72.0 kips and span lengths ranging from 10 to 100 feet. These maximum moments can be related to stress range and the property (Z/L) , section modulus divided by span length. A relationship between N_f , α and (Z/L) is then obtained by applying Eqs. (11) and (12), which give for span length ranges:

$$0 \leq L \leq 40',$$

$$\text{Log } N_f = 9.158 - 2.98 \text{Log} \left(\frac{K_1}{Z/L} \right), \tag{13}$$

$$\text{Log} (\alpha - 1) = 1.634 - 0.87 \text{Log} \left(\frac{K_1}{Z/L} \right), \tag{14}$$

$$40' \leq L \leq 100',$$

$$\text{Log } N_f = 9.158 - 2.98 \text{Log} \left(\frac{\bar{K}}{Z/L} \right), \tag{15}$$

$$\text{Log} (\alpha - 1) = 1.634 - 0.87 \text{Log} \left(\frac{\bar{K}}{Z/L} \right), \tag{16}$$

where K_1 and \bar{K} are constants as established for the given truck types. A plot of Eqs. (13) through (16), considering upper and lower bounds on \bar{K} , yields

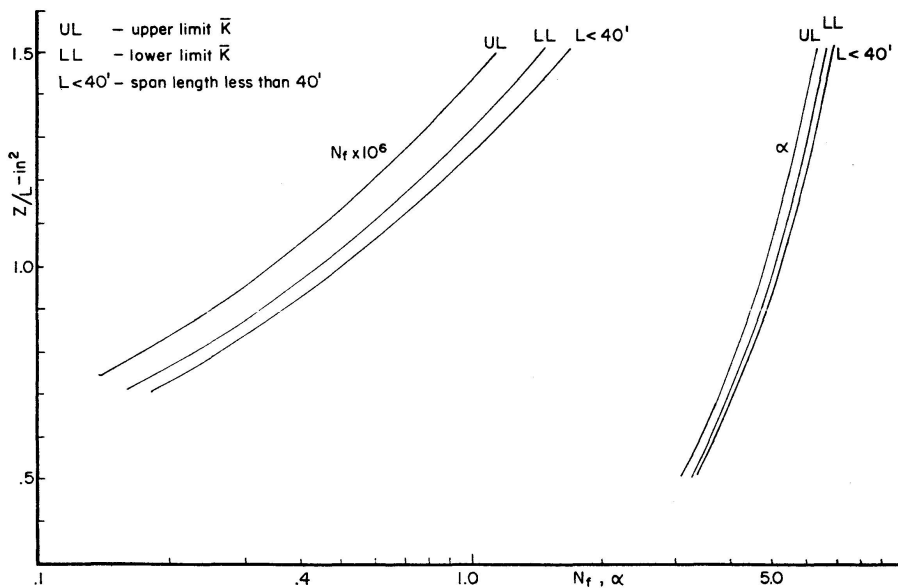


Fig. 11. N_f, α Curves for 2 D Truck Type.

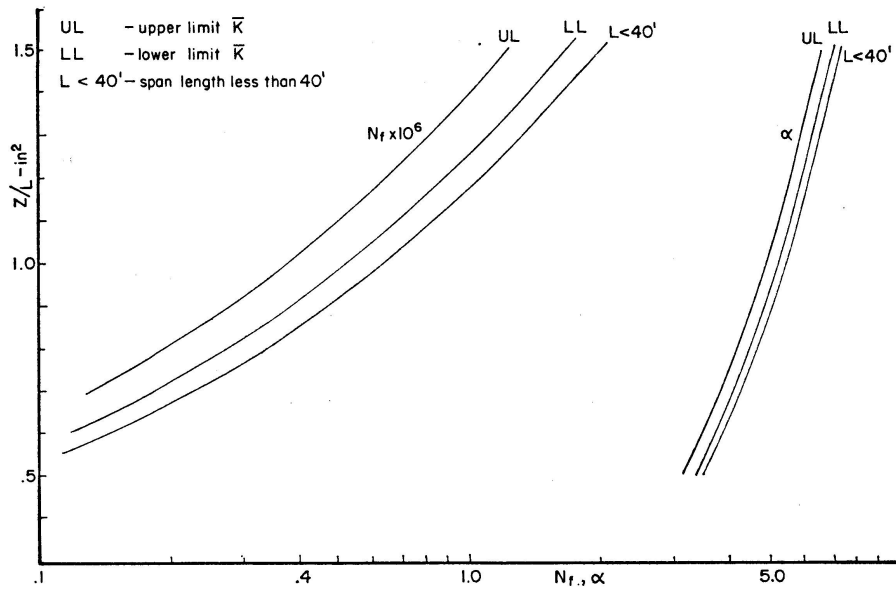


Fig. 12. N_f, α Curves for 3 Truck Type.

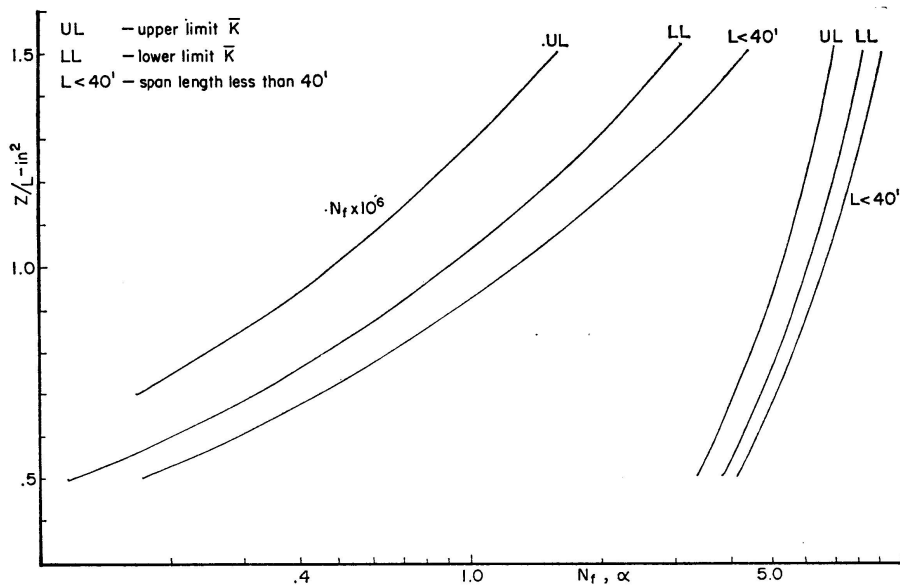


Fig. 13. N_f, α Curves for 2 S-1 Truck Type.

Figs. 11 through 15. These curves can then be applied in conjunction with particular load patterns, as described previously.

It should be noted that all of these curves are for vehicles whose gross weight equals 72.0 kips. The values obtained from these curves or Eqs. (13) and (14) should be multiplied by the factor $(72/GW/DF)^{2.98}$ and Eqs. (15) and (16) by the factor $(72/GW/DF)^{0.87}$, for other gross weights where (GW) represents the gross weight and (DF) equals the distribution factor.

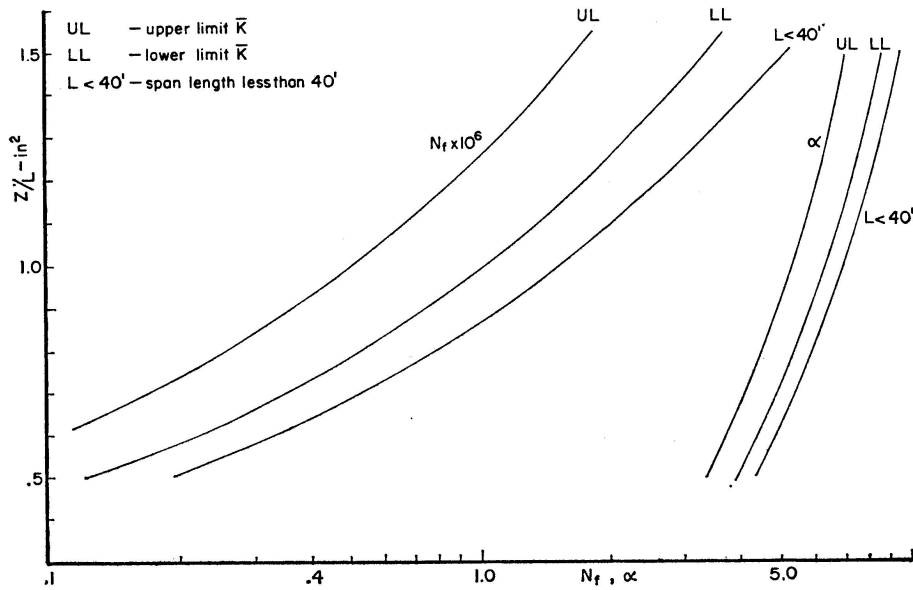


Fig. 14. N_f, α Curves for 2 S-2 Truck Type.

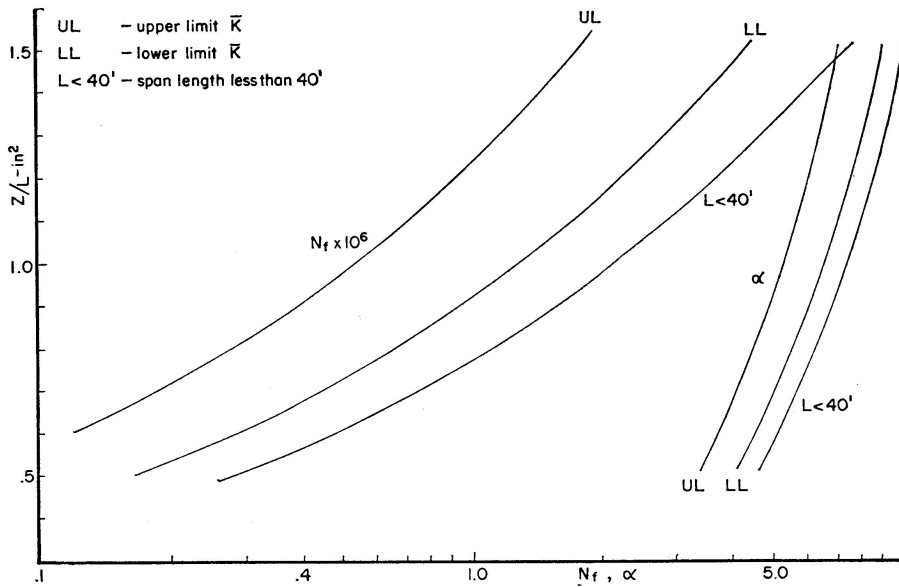


Fig. 15. N_f, α Curves for 3 S-2 Truck Type.

Notations

- A* a stress dependent material constant
- b* intercept of $\text{Log } \sigma_r$ vs. $\text{Log } N_f$ equation
- c* slope of $\text{Log } \sigma_r$ vs. $\text{Log } N_f$ equation
- d* intercept of $\text{Log } (\alpha - 1)$ vs. $\text{Log } \sigma_r$ equation
- e* slope of $\text{Log } (\alpha - 1)$ vs. $\text{Log } \sigma_r$ equation
- D* damage
- D_i* damage due to n_i cycles

K, K_1	constants
N_f	number of constant amplitude cycles to failure
n	number of consecutive cycles
\bar{n}	equivalent number of cycles
n/N_f	cycle ratio
\bar{n}/N_f	equivalent cycle ratio
S	standard deviation
α	a stress dependent material constant
ϵ_p, ϵ	accumulated plastic strain at n cycles
ϵ_f	accumulated strain at failure
$d\epsilon_p/dn$	accumulated strain per cycle
γ	a stress dependent material constant
σ_r	stress range at cover plate end, except as noted

Acknowledgements

The analytical and experimental studies contained herein are part of a research project sponsored by the Maryland State Roads Commission and the U.S. Bureau of Public Roads. Their guidance and help is gratefully acknowledged.

Bibliography

1. "Loading Histories of Highway Bridges, Program to Gather Field Data." Information from Structures and Applied Mechanics Division, Office of Research and Development, U.S. Bureau of Public Roads, March 1, 1968.
2. Highway Research Circular # 61, Highway Research Board, Research Problem # 76, # 60, January 1967.
3. "A Strain History Data System for Use on Highway Bridges." C. F. Galambos, BPR Washington, D.C., HRB January 1967.
4. "Loading History of Highway Bridges." C. F. Galambos, W. L. Armstrong, BPR Washington, D.C., HRB January 1969.
5. "Induced Dynamic Strains in Bridge Structures due to Random Truck Loadings." M. W. Novak, C. P. Heins, C. T. G. Looney, Civil Engineering Dept., University of Maryland, College Park, Md., Feb. 1968, Rept. No. 18.
6. "Tabulation of 24 Hour Dynamic Strain Data on Four Simple Span Girder-Slab Bridge Structures." C. P. Heins, Jr., Arthur D. Sartwell, Civil Engineering Dept., University of Maryland, College Park, Md., June 1969, Rept. No. 29.
7. Tabulation of Dynamic Strain Data on a Three Span Continuous Bridge Structure." A. D. Sartwell, C. P. Heins, Jr., Civil Engineering Dept., University of Maryland, College Park, Md., Nov. 1969, Rept. No. 33.
8. "Tabulation of Dynamic Strain Data on a Girder-Slab Bridge Structure During Seven Continuous Days." A. D. Sartwell, C. P. Heins, Jr., Civil Engineering Dept., University of Maryland, College Park, Md., Sept. 1969, Rept. No. 31.
9. "Elastic Hysteresis Property of Several Steels under Fatigue Load." Kawamoto, M., Tanaka, T., Trans. Japan Society of Mechanical Engineers, 1965.

10. "Processes of Creep and Fatigue in Metals." A. J. Kennedy, John Wiley, N. Y., 1963.
11. "Effect of Weldments on Fatigue Strength of Steel Beams." J. W. Fisher et al., Lehigh Univ., Bethlehem, Pa., Sept. 1969, Fritz Lab. Rept. No. 334.2.
12. "Fatigue of Beams with Welded Cover Plates." F. A. Murad, C. P. Heins, Civil Engineering Dept., University of Maryland, College Park, Md., Sept. 1970, Rept. No. 38.
13. "Cumulative Damage in Fatigue." M. A. Miner, J. Appl. Mech. Vol. 12, No. 1, Sept., 1945.
14. "A Theory of Fatigue-Damage Accumulation in Steel." D. L. Henry, Trans. ASME, Vol. 77, No. 6, Aug. 1955.

Summary

The fatigue life of steel beams with welded cover plates is predicted by a strain accumulation damage theory. The theory permits application of random loads, thus considers load order. The resulting equations are applied to the response of five typical truck types on a simple span of varying lengths.

Résumé

La résistance à la fatigue de poutres en acier avec des couvre-joints soudés est déterminée à l'avance grâce à la théorie des déformations et des détériorations. La théorie permet l'application de charges supplémentaires et tient compte de leur ordre de grandeur. Les équations qui en résultent sont alors appliquées au comportement de cinq types de véhicules sur une ouverture simple de portée variable.

Zusammenfassung

Die Ermüdungsdauer von Stahlträgern mit geschweissten Deckplatten wird mittels einer Verformungs-Schadentheorie vorausbestimmt. Die Theorie gestattet die Anwendung von Zusatzbelastungen und zieht so die Grösse der Belastung in Betracht. Die sich ergebenden Gleichungen werden auf das Verhalten von fünf Typen von Fahrzeugen auf einfache Öffnungen variabler Länge angewandt.

Leere Seite
Blank page
Page vide